J MATER SCI **41** (2006) 4365–4372

Methods for modelling the ultimate strength of orthotropic plate with a central hole under uniaxial tension

S. BASELGA ARIÑO*, M. MAZA FRECHÍN
Department of Mechanical Engineering, University of Zaragoza, St/María de Luna, s/n, (Betancourt), 50018 Zaragoza, Spain
E-mail: sbaselga@unizar.es

Published online: 15 June 2006

The stress state in plates with circular holes made of orthotropic homogeneous material has no singularities and it can be exactly determined. The numerical stress distribution calculation by the finite element method will be compared with those obtained by the analytical equations developed by several authors.
The goal of this work is to validate the finite element method, in conjunction with in-plane and out of plane failure criteria, in order to calculate not only the stress distribution for orthotropic plates with circular holes but also to determine their ultimate strength.
The tool used has been a user subroutine (UMAT) specially developed for this work that implements the features of the commercial FE program (ABAQUS). The code performs an implicit analysis of the stress-state with progressive damage modelling.
Finally, both of them, numerical and analytical method, will be checked with experimental tests by means of strain gauges.

1. Introduction

It is important to point out the work performed by Konish, Whitney, Nuismer, Gillespie, Lekhnitskii and other authors who developed analytical expressions for the calculation of stress distributions in plates with circular holes.

The results obtained with finite elements method will be compared with those obtained from the referenced authors and they will be correlated with the measurements from strain gauges placed on real specimens subjected to the same load and boundary conditions.

In relation with the ultimate strength, our study is supported by the work carried out by Chang [1–3] who presented three different in-plane failure modes and their respective material degradations. The interlaminar failure mode will be added in order to determine its relative importance.

In this work we will also determine the characteristic dimension (a_o) of the average stress criterion (A.S.C.) developed by Whitney [9, 12], for our particular material. Finally, a useful new entity called (design coefficient) is getting out. It enables to know the tendency of strength reduction in a plate with a centred hole, and so, it saves time in further calculations.

2. Analytical expressions

Lekhnitskii [7] developed an analytic model for orthotropic plates with centred circular holes. On the basis of this model of Lekhnitskii, the stress profile at the edge of the hole represented in Figs 1 and 2 is:

$$\sigma_\vartheta = P\left(\frac{E_\vartheta}{E_x}\right)\{[-\cos^2\varphi + (K+n)\sin^2\varphi] \times K\cos^2\vartheta + [(1+n)\cos^2\varphi - K\sin^2\varphi] \times \sin^2\varphi - n(1+K+n) \times \sin\varphi\cos\varphi\sin\vartheta\cos\vartheta\} \quad (1)$$

where:

$$K = \sqrt{\frac{E_x}{E_y}} \quad (2)$$

$$n = \sqrt{2\left(\sqrt{\frac{E_x}{E_y}} - \nu_{xy}\right) + \frac{E_x}{G_{xy}}} \quad (3)$$

*Author to whom all correspondence should be addressed.

0022-2461
DOI: 10.1007/s10853-006-7950-4

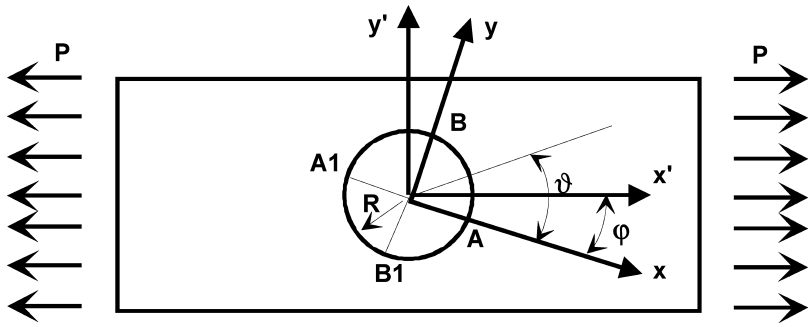

Figure 1 Orthotropic plate with circular hole (z axis view).

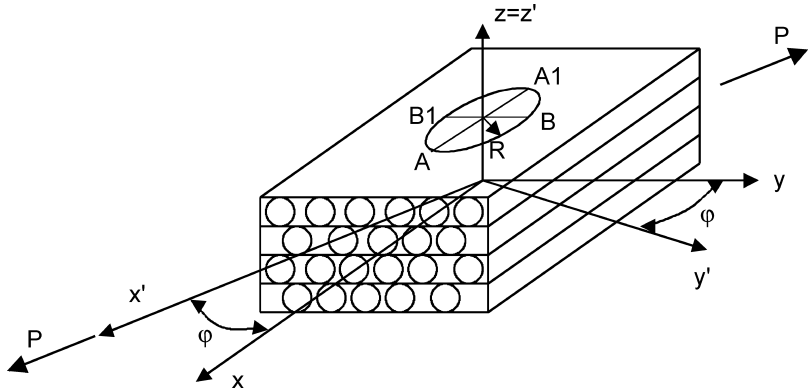

Figure 2 Orthotropic plate with circular hole (general view).

When the load is applied in the direction of the principal orthotropic axis (x) (for example the axis coincident with de orientation of the fibres in a unidirectional laminate), the stresses at points (B) and (B1), (Figs 1 and 2) which are located in the diameter perpendicular to the load direction, will have the known form:

$$\sigma_\vartheta = P\,(1+n) = P\,K_t^\infty \tag{4}$$

where $(K_t^\infty = 1+n)$ is the stress-concentration factor for an infinite plate.

Gillespie in his article "Influence of finite width on notched laminate strength predictions" [4] explains: "A common method used extensively in the literature to relate experimental notched strength (σ_N), for plates of finite width to the notched strength of plates of infinite width is to simply multiply (σ_N) by a correction factor (K_t/K_t^∞)". Thus, the expression that quantifies the new ultimate tensile strength taking account of the finite width of the specimen will be:

$$\sigma_N^\infty = \sigma_N \left(\frac{K_t}{K_t^\infty}\right) \tag{5}$$

$\sigma_N^\infty =$ Ultimate tensile strength for an infinite plate with a circular hole, $\sigma_N =$ Ultimate tensile strength for a finite plate with a circular hole, $K_t^\infty =$ Stress-concentration factor for an infinite plate, $K_t =$ Stress-concentration factor for a finite plate

Following the Gillespie indications at the mentioned article [4], it has been proposed that an isotropic expression for (K_t/K_t^∞) can be used for orthotropic materials as well,

$$\frac{K_t}{K_t^\infty} = \frac{2+\left(1-\frac{D}{W}\right)^3}{3\left(1-\frac{D}{W}\right)} \tag{6}$$

where (see Fig. 3), $R =$ Hole Radius, $D = 2\mathrm{R} =$ Hole diameter $W =$ Plate Width

Inherent to this procedure is the assumption that the entire stress distribution ($\sigma_x(0,y)$) in a finite plate within the highly stressed region defined by ($R \le y \le W/2$) scales with the parameter (K_t/K_t^∞), then:

$$\frac{\sigma_x\,(0,\,y)}{\sigma_x^\infty\,(0,\,y)} = \frac{K_t}{K_t^\infty} = \text{constant} \tag{7}$$

where$(\sigma_x^\infty(0,\,y))$ is the normal stress distribution in an infinite plate.

According to the studies performed by Konish and Whitney [6], the approximated normal stress distribution for an infinite orthotropic plate with a central hole of radius (R) subjected to traction load in the principal direction (X) is for ($y \ge R$) (Fig. 3):

$$\sigma_x^\infty(0,\,y) = \frac{\sigma_x^\infty}{2}\left\{2+\left(\frac{R}{y}\right)^2+3\left(\frac{R}{y}\right)^4\right.$$

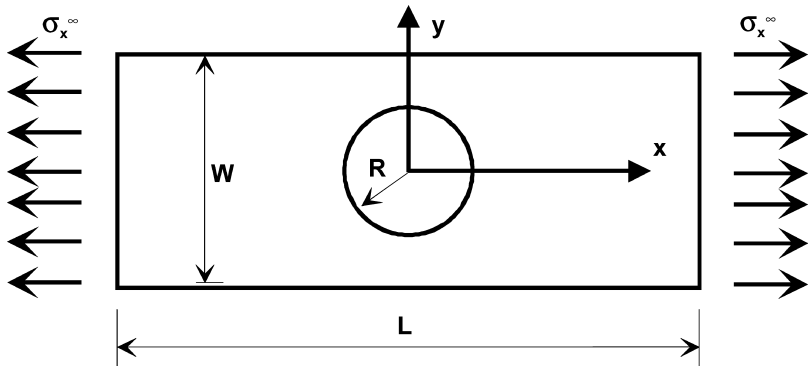

Figure 3 Axes of reference.

$$-(K_t^{\infty}-3)\left[5\left(\frac{R}{y}\right)^6-7\left(\frac{R}{y}\right)^8\right]\Bigg\} \qquad (8)$$

where(σ_x^{∞}) is the stress far away from the hole: $(\sigma_x^{\infty} = \sigma_x^{\infty}(L/2, y))$.

For laminates with $(W/\mathrm{D} \leq 4)$, $(\sigma_x(0, y)/\sigma_x^{\infty}(0, y))$ is a decreasing function of (y), with the slope of the relation being dependent on orthotropy and (W/D). Consequently, the finite width correction factor is only valid at the hole edge $(y = R)$ and significant error accumulates as the distance from the hole boundary increases.

To improve the representation of stress profile adjacent to the hole where fracture initiates a non-dimensional function $(\delta(y))$ is introduced, so that the finite width stress profile will be expressed in the following form:

$$\frac{\sigma_x(0, y)}{\sigma_x^{\infty}(0, y)} = \frac{K_t}{K_t^{\infty}}(1+\delta(y)) \qquad (9)$$

The function $(\delta(y))$ defined in Equation 9, quantifies the relative divergence of the actual width stress profile, and it can be approximated as:

$$\delta(y) = -C(y-R)\left(\frac{K_t}{K_t^{\infty}}-1\right) \qquad (10)$$

With the following boundary conditions:

$$(\delta(y=R)=0); \quad (-1 \leq \delta(y>R) \leq 0)$$

(C) is the slope, and it depends of the material. In his paper "Influence of finite width on notched laminate strength predictions" [4] Gillespie suggest taking a value of (C) approximately equal to $(70\ \mathrm{m}^{-1})$. As first approximation, we are going to keep this value for orthotropic materials. If a further calculation by the finite element analysis shows great discrepancies, the value of (C) can be changed to obtain better approximations of the stress state. Otherwise, this value keeps as $(70\ \mathrm{m}^{-1})$.

3. Failure criteria

The failure criteria selected are:

(a) Average stress criterion (A.S.C.) for the analytical calculations.

The A.S.C. was proposed by Nuismer and Whitney [9, 12]. It assumes that failure occurs when the average stress value of (σ_x) over some fixed distance (a_o), ahead of the notch first reaches the unnotched tensile strength of the material; for the circular hole, failure occurs when:

$$\frac{1}{a_o}\int_R^{R+a_o}[\sigma_x(0, y)]\mathrm{d}y = \sigma_o \qquad (11)$$

This criterion has got an unknown parameter (a_o), which depends on the material, the laminate and the geometry of the plate.

b) Progressive damage criteria for the Finite Element Analysis.

They are the most appropriate to be use in the calculation through the finite element technique with sequential progressive load.

There are different independent modes of failure. With all of them we take account of the in-plane and out of

TABLE I Degradation criteria with in-plane matrix cracking

$(E_x)_{n+1} = E_x$	$(G_{xy})_n = G_{xy}$	$(\nu_{xy})_n = \nu_{xy}$
$(E_y)_{n+1} = d_3(E_y)_n$	$(G_{xz})_n = G_{xz}$	$(\nu_{xz})_n = \nu_{xz}$
$(E_z)_{n+1} = d_3(E_z)_n$	$(G_{yz})_{n+1} = d_3(G_{yz})_n$	$(\nu_{yz})_{n+1} = d_3(\nu_{yz})_n$

TABLE II Degradation criteria with in-plane fiber-matrix shearing failure

$(E_x)_n = E_x$	$(G_{xy})_{n+1} = d_g(G_{xy})_n$	$(\nu_{xy})_n = \nu_{xy}$
$(E_y)_{n+1} = \mathrm{d_g}^2(\mathrm{E_y})_n$	$(\mathrm{G_{xz}})_{n+1} = \mathrm{d_g}(G_{xz})_n$	$(\nu_{xz})_n = \nu_{xz}$
$(E_z)_{n+1} = \mathrm{d_g}^2(E_z)_\mathrm{n}$	$(\mathrm{G_{yz}})_{n+1} = \mathrm{d_g}^2(G_{xz})_n$	$(\nu_{yz})_{n+1} = d_g{}^2(\nu_{yz})_n$

TABLE III Degradation criteria with in-plane fibre breakage

$(E_x)_{n+1} = d(E_x)_n$	$(G_{xy})_{n+1} = d(G_{xy})_n$	$(\nu_{xy})_{n+1} = d(\nu_{xy})_n$
$(E_y)_{n+1} = d_g{}^2(E_y)_n$	$(G_{xz})_{n+1} = d(G_{xz})_n$	$(\nu_{xz})_{n+1} = d(\nu_{xz})_n$
$(E_z)_{n+1} = d_g{}^2(E_z)_n$	$(G_{yz})_{n+1} = d_g{}^2(G_{yz})_n$	$(\nu_{yz})_{n+1} = \mathrm{d_g}^2(\nu_{yz})_n$

TABLE IV Degradation criteria with interlaminar failure

$(E_x)_n = E_x$	$(G_{xy})_n = G_{xy}$	$(\nu_{xy})_n = \nu_{xy}$
$(E_y)_n = E_y$	$(G_{xy})_{n+1} = d_i(G_{xz})_n$	$(\nu_{xz})_{n+1} = d_i(\nu_{xz})_n$
$(E_z)_{n+1} = d_i(E_z)_n$	$(G_{yz})_{n+1} = d_i(G_{yz})_n$	$(\nu_{yz})_{n+1} = d_i(\nu_{yz})_n$

TABLE V Stiffnes properties of a layer in the principal directions

$E_x = 36150$ Mpa	$G_{xy} = 4230$ Mpa	$\nu_{xy} = 0.26$
$E_y = 8560$ Mpa	$G_{xz} = 4230$ Mpa	$\nu_{xz} = 0.26$
$E_z = 8560$ Mpa	$G_{yz} = 2930$ Mpa	$\nu_{yz} = 0.5$

TABLE VI Ultimate strength of a layer in the principal directions

$X = 440$ Mpa	$S_{xy} = 39$ Mpa
$X' = 130$ Mpa	$S_{xz} = 39$ Mpa
$Y = 70$ MPa	$S_{yz} = 34$ Mpa
$Y' = 80$ Mpa	
$Z = 70$ Mpa	
$Z' = 80$ Mpa	

TABLE VII Geometrry of the specimens

1) Specimen 1:	$W/D = 12$	$W = 0.060$ m
2) Specimen 2:	$W/D = 8$	$W = 0.040$ m
3) Specimen 3:	$W/D = 4$	$W = 0.020$ m
4) Specimen 4:	$W/D = 2$	$W = 0.010$ m

plane failure. The Young's moduli, Poisson's ratios and shear moduli have to be reduced according to the failure modes which damage the plies in a similar manner than the model from Nguyen [8].

(d), (d_g), (d_1), (d_2) and (d_3), are degradation parameters. It will be explained how to use them in Tables I–IV. These parameters keep constant when the failure occurs but the properties affected decreases progressively in each step of the sequential calculation from $n = 1$ to $n = n_f$.

$(n = 1)$ is the first step of the sequential calculation when initial failure occurs

$(n = n_f)$ is the last step of the sequential calculation when final failure occurs

The new elastic properties of the degraded material are denoted by the $(xx)_n$ notation in Tables I–IV, whereas the others without brackets are the properties of the intact material.

b1) In-plane matrix cracking. The criterion has the form:

$$\left(\frac{\sigma_y}{Y}\right)^2 + \left(\frac{\tau_{xy}}{S_c}\right)^2 = e_m^2 \tag{12}$$

where σ_y = Transverse tensile stress in each layer, τ_{xy} = Shear stress in each layer, Y = In-plane transverse normal strength in each layer, S_C = In-plane shear strength in each layer, (x, y, z) are the principal axes of the unidirectional layer. (x) is the axis in the direction of the fibre (Fig. 4).

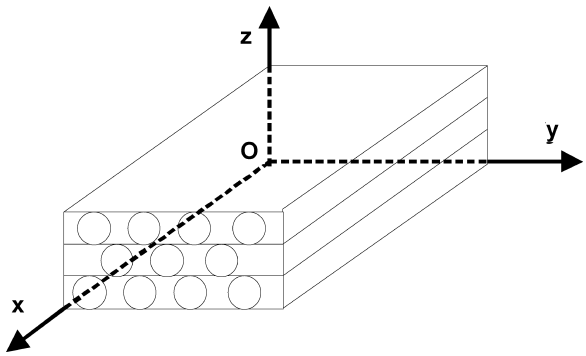

Figure 4 Principal directions of the laminate.

If $(e_m \geq 1)$, it is assumed that matrix cracking occurs and thus, the properties will be degraded according to the following expressions:

Where (d_3). is a degradation parameter. An example of the value taken for (d_3) will be showed later in this paper.

b2) In-plane fiber-matrix shearing. The criterion is expressed by:

$$\left(\frac{\sigma_x}{X}\right)^2 + \left(\frac{\tau_{xy}}{S_c}\right)^2 = e_f^2 \tag{13}$$

With $\left|\frac{\sigma_x}{X}\right| < \left|\frac{\tau_{xy}}{S_c}\right|$ and $\left|\frac{\sigma_x}{X}\right| < 1$, σ_x = Longitudinal tensile stress in each layer, X = In-plane longitudinal normal strength in each layer

If $(e_f \geq 1)$, fiber-matrix shearing occurs and thus, the properties will be degraded according to the following expressions:

Where (d_g) is a degradation parameter. An example of the value taken for (d_g) will be showed later in this paper.

b3) In-plane fibre breakage. The criterion has the form:

$$\left(\frac{\sigma_x}{X}\right)^2 + \left(\frac{\tau_{xy}}{S_c}\right)^2 = e_f^2 \tag{14}$$

with $\left|\frac{\sigma_x}{X}\right| \geq \left|\frac{\tau_{xy}}{S_c}\right|$

If $(e_f \geq 1)$, fiber-matrix shearing occurs and thus, the properties will be degraded according to the following expressions:

(d) and (d_g) are degradation parameters. An example of the values taken for (d) and (d_g) will be showed later in this paper.

b4) Interlaminar failure. The criterion has the form:

$$\left(\frac{\sigma_z}{Z}\right) + \left(\frac{T}{S}\right)^2 = e_i \tag{15}$$

with, $T^2 = \tau_{xz}^2 + \tau_{yz}^2$, Where: σ_z = Interlaminar normal stress, τ_{xz} = Interlaminar shear stress in the load direction, τ_{yz} = Interlaminar shear stress transverse to the load direction, Z = Interlaminar normal strength (tensile or compressive), S = Interlaminar shear strength.

If ($e_i \geq 1$), it is assumed that matrix cracking occurs and thus, the properties will be degraded according to the following expressions:

$$(d_i = d_1 \text{ when } \sigma_z < 0) \text{ and } (d_i = d_2 \text{ when } \sigma_z \geq 0).$$

(d_1) and (d_2) are degradation parameters. An example of the value taken for (d_i) will be showed later in this paper.

As it is obvious, when the layer is not unidirectional, the degradation of the material elastic properties must be adapted to the kind of layer.

4. Stress distributions

The material used is:

Resin: epoxy (DOW-DER 335), Fibre: ARAMIDE (Kevlar-49)

Fabrication Process: Vacuum bag moulding, $V_f = 28\%$

Ply: Unidirectional ply thickness: 0.000285 m

Lay-up: $[0]_{16}$ Total thickness: 0.00456 m.

These specimens were made in our laboratory, and experimentally tested in it following the classical methods to obtain their mechanical properties. In consequence, these material properties belong to our own material which was obtained by vacuum bag moulding.

The mechanical properties of a layer in the principal direction are given in Tables V and VI.

The geometry of the specimens is shown in Fig. 5. The following dimensions are kept constant:

$L = 0.250$ m., $l = 0.050$ m., $D = 0.005$ m., $t = 0.003$ m., $e = 0.00456$ m., $\alpha = 30^\circ$

In order to study the influence of the width, the ratios in Table VII are selected.

The strain gauges were placed on all the specimens as depicted in Fig. 6. The characteristics of the gauges are:

Length = 0.001m, Width = 0.0007mm.,

R = 120 ± 0.3 Ω, Gauge factor = 2.1

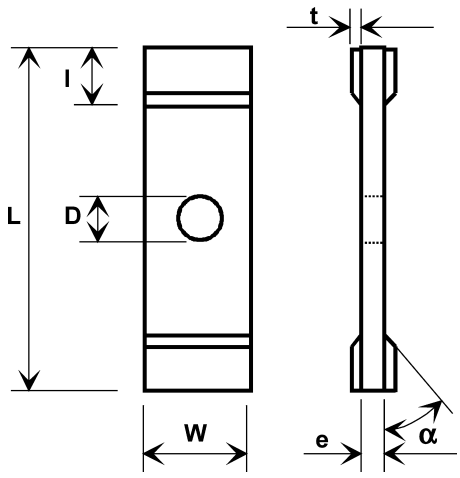

Figure 5 Specimen geometry.

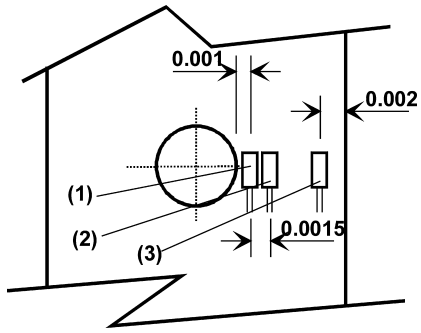

Figure 6 Strain gauges disposition.

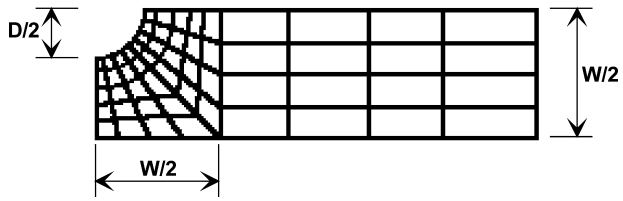

Figure 7 Mesh of the plate.

A quasi-static increasing traction load is applied in the principal direction (x) as it is represented in Fig. 3, where (σ_x^∞) is the stress far away from the hole:

$$(\sigma_x^\infty = \sigma_x^\infty(L/2, y)).$$

To avoid the analysis of the thermal stresses as a parameter of study with different influence in each specimen, we worked with the next premises; the temperature conditions while the test are going to be kept constant for all of them and the manufacturing of the specimens for testing was done in similar ambient conditions.

Three repetitions by test were carried out.

As it was explained above, we are going to solve the stress distribution by using the finite element method. We selected the standard parabolic volumetric element with 20 nodes from the (ABAQUS) library. The kind of mesh is shown in Fig. 7.

The Length of the elements decreases proportionally as the element is closer to the hole edge.

We begin with 200 elements at the first step of the convergence study and we increment 200 elements in each of the next calculation. We are going to check a point on the hole edge subjected to a load such that there is no failure in any place of the specimen. In this situation the behaviour of the material is elastic-linear. The results of the convergence study are reflected in Fig. 8, where (σ_C) is stress obtained by the F.E.M. and (σ_T) is the analytical stress. As it can be realized, (σ_C/σ_T) grows when the number of elements increases from a minimum of 200 and has a tendency of stabilization with 800 elements or more.

From the previous study, the number of degrees of freedom of the selected modelization is greater than 6000. Taking advantage of the loads symmetry and geometry,

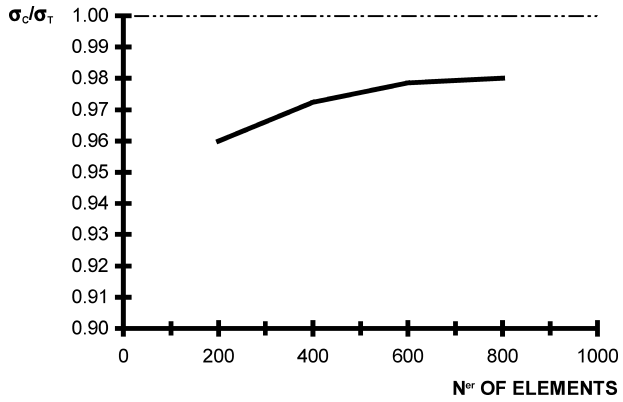

Figure 8 Convergence study.

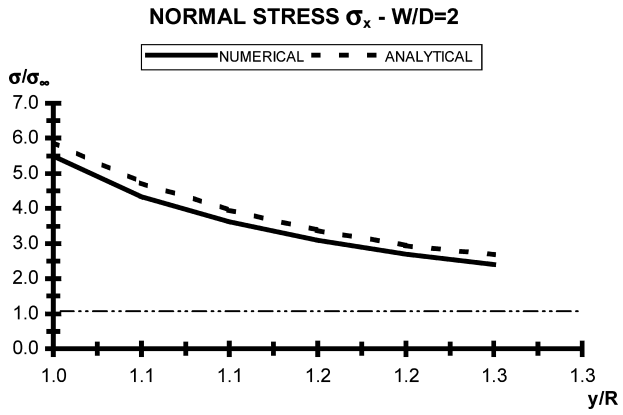

Figure 9 Correlation analytical (Gillespie)-numerical (F.E.M.). $W/D = 2$.

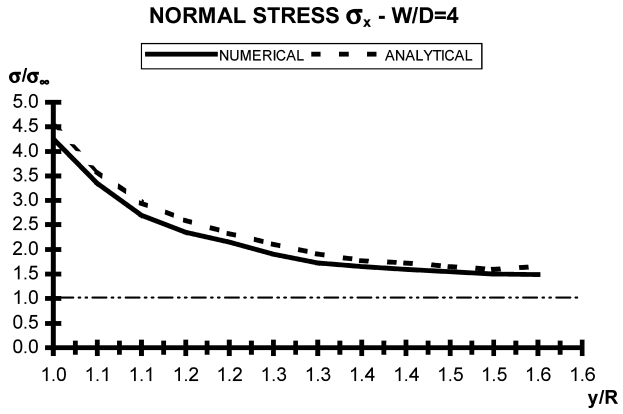

Figure 10 Correlation analytical (Gillespie)-numerical (F.E.M.). $W/D = 4$.

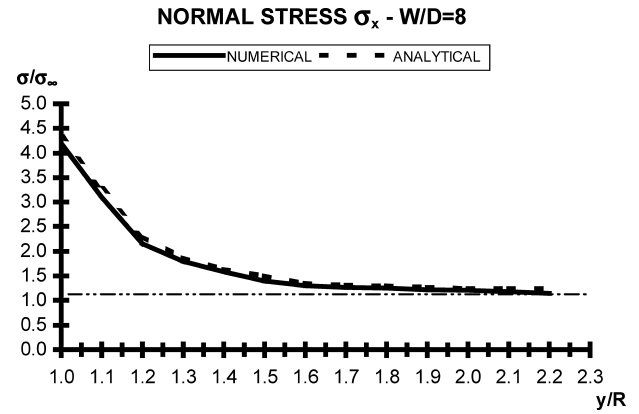

Figure 11 Correlation analytical (Gillespie)-numerical (F.E.M.). $W/D = 8$.

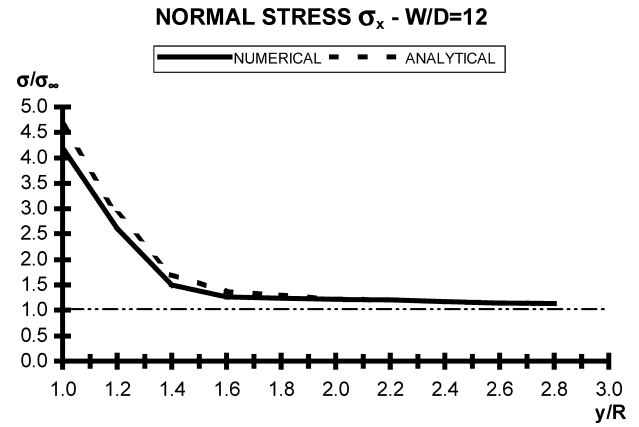

Figure 12 Correlation analytical (Gillespie)-numerical (F.E.M.). $W/D = 12$.

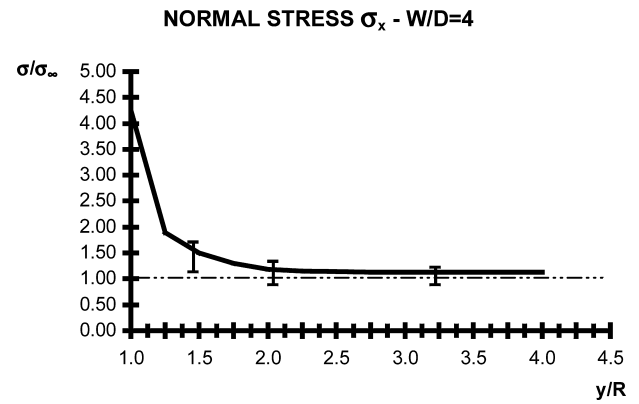

Figure 13 Correlation numerical (F.E.M.)-experimental, $W/D = 4$.

only 1/8 of the specimen was meshed which saved computing time.

The normal stress (σ_x) in the direction perpendicular of the load at ($x = 0$) is plotted at Figs 9–12. The results obtained by both methods, analytical and numerical, are compared in those graphics. It can be observed that analytical and numerical stresses correspond very well at the points with the highest stress gradients, so there seems to be a good correlation between both methods of calculation.

The range of variation of the stresses experimentally obtained with the gauges is plotted at the Figs 13 and 14. As Table VIII shows, the data provided from the gauges give average errors less than 12% with respect to the numerically predicted stresses.

5. Ultimate strength

As it has been demonstrated, and taking into account that the Gillespie's method is correct, the finite element

TABLE VIII Correlation F.E.M.-Experimental

		$\sigma_x(0,y)/\sigma_x^{\infty}(L/2,y)$					
W/D	N^{er} rep	Gauge (1) $y=0.0035$ m	Average error (%)	Gauge (2) $y=0.005$ m	Average error (%)	Gauge (3) $y=$ W/2-0.002 m	Average error (%)
4	3	1.36	7.5	1.16	9.4	1.07	2.7
8	3	1.31	12.2	1.10	8.3	1.02	7.3
12	3	1.25	11.9	1.10	7.5	1.02	2.8

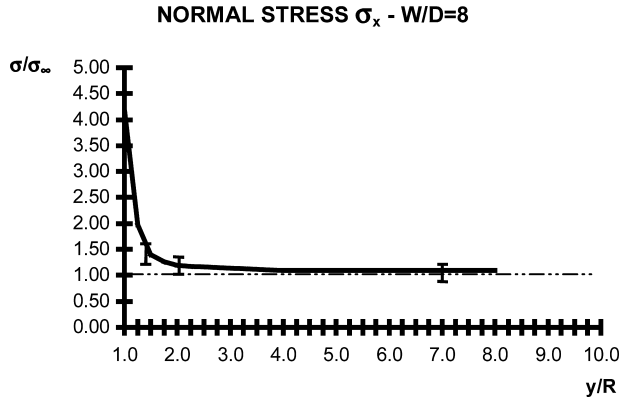

Figure 14 Correlation numerical (F.E.M.)-experimental, $W/D=8$.

method developed before gives good results when no failure occurs. Our goal is now to obtain the ultimate failure load using the FEM with non-linearities due to progressive degradation of the material mechanical properties when it fails.

The calculations were done with the implicit module of the commercial code (ABAQUS). The load was applied step by step from null to ultimate failure load. In each step the program calculated the strains. Next, we used our own subroutine (UMAT) for the stresses calculation and to apply the different criteria on each element stress state. When an element fails, its elastic properties are degraded in all the next steps.

The selected initial values for the degradation parameters are:

Fibre breakage: $d=0.05$

Fibre-matrix shear: $d_g=0.80$

Interlaminar failure with compression stress: $d_1=0.70$

Interlaminar failure with tensile stress: $d_2=0.10$

Matrix cracking: $d_3=0.20$

These initial values can be adjusted for each material when the results obtained in the experimental test differ considerably. As long as we have more tests with different materials we can obtain a general data base.

Matrix cracking appears at the hole edge at 26° from the load direction. The area damaged by shear stresses increases, but the ultimate failure is due to the breakage of the fibres subjected to tensile stress. In this material there are no interlaminar failures.

The ultimate failure loads takes place when in the considered step of the implicit module of (ABAQUS) there is no convergence and stops of calculations occur. The results obtained are shown in Table IX.

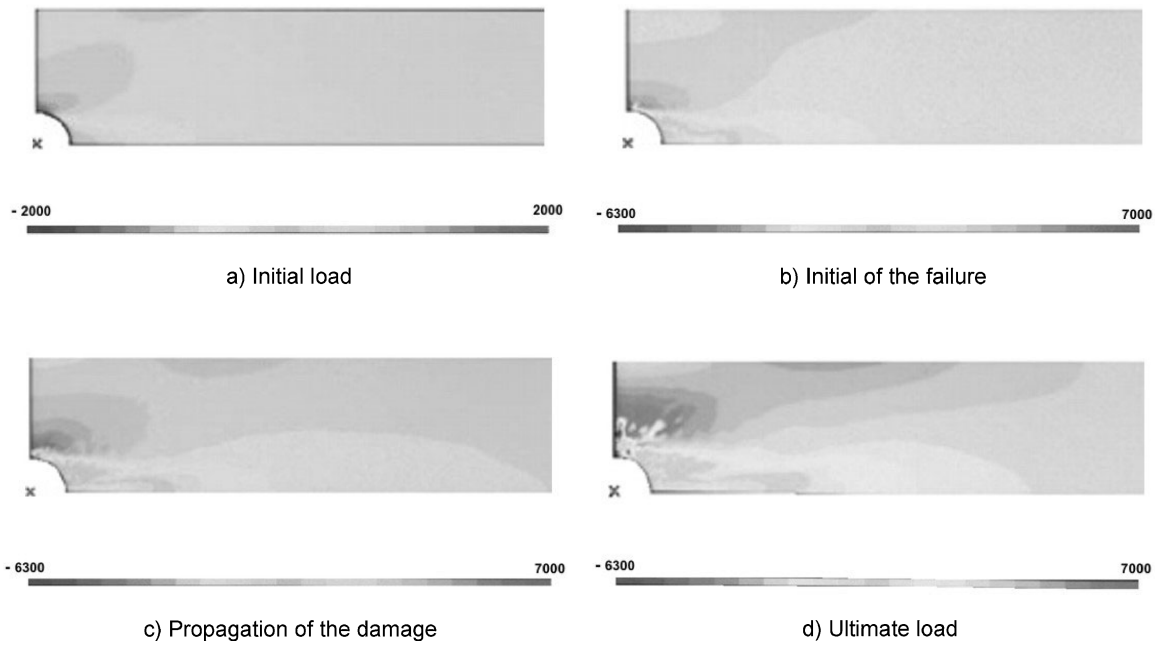

Figure 15 σ_x stress distribution, $(W/D)=4$.

TABLE IX Ultimate load

	σ_x^{∞} ultimate (MPa)			
W/D	Numerical	Experimental	Average error (%)	K_d
2	105	115	8.7	3.826
4	205	210	2.4	2.095
8	225	240	6.2	1.833
12	275	260	5.8	1.692

TABLE X Characteristic length, stress concentration factor and design coefficient

W/D	a_o (m)	d_o (m)	K_t	K_t
2	0.000584	0.000248	5.8816	3.826
4	0.001625	0.000559	4.4688	2.095
8	0.002066	0.000669	4.2227	1.833
12	0.002540	0.000780	4.1822	1.692

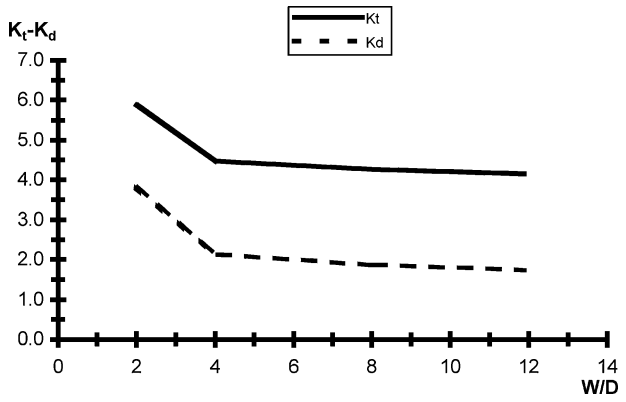

Figure 16 Stress concentration factor (K_t) and design coefficient (K_d).

The coefficient (K_d), which we have called (design coefficient), quantifies the strength reduction of a plate with a centred circular hole, with respect to the same intact plate when it is subjected to traction load in the principal direction (x).

The dependence of the design coefficient and the stress concentration factor with the (W/D) ratio is represented in Fig. 16. The results show that (K_t) and (K_d) have small variations for infinite plates ($W/D \geq 12$), but they have large increases for ($W/D < 4$).

Finally, the characteristic length of the A.S.C. (a_o) given in Table X, increases as the (W/D) ratio increase.

6. Conclusions

For the material and geometries of the specimen analysed, the F.E.M. appears to be a good calculation method with errors lower than 12% with respect to the experimental results.

It is possible that some of the errors are due to the difficulty in placing the gauges, thus it shall be convenient to contrast the results with another experimental method as Moire Technique.

The results obtained by both methods, analytical and numerical agree quite well at the points with the highest stress gradients, so there seems to be a good correlation between both calculation methods.

For the material and geometries of the specimen analysed, the progressive damage criterion seems to be an acceptable criterion for the strength calculation when there is stress concentration.

Finally, as the (design coefficient) quantifies the strength reduction of the plate due to the existence of a circular hole, the results obtained from the studied material can be used. This simplify the calculation process of orthotropic plates that have different (W/D) ratios without the necessity to develop the complete analytical method of calculation. The design coefficient is dependent on the material and the geometry of the plate, thus it has to be experimentally determined in order to obtain a data base for all materials.

References

1. F. K. CHANG and K. Y. CHANG, *J. Comp. Mat.* **21** (1987) 834.
2. F. K. CHANG, L. LESSARD and J. M. TANG, *SAMPE Quarterly* **19** (1988) 46.
3. K. Y. CHANG, S. LIU and F. K. CHANG, *J. Comp. Mat.* **25** (1991) 274.
4. J. W. GILLESPIE JR and L. A. CARLSSON, *Comp. Sci. Tech.* **32** (1988) 15.
5. KARLSSON, HIBBITT and SORENSEN, Inc., 'ABAQUS Manuals'. Version 5.8., 1998.
6. H. J. KONISH and J. M. WHITNEY, *J. Comp. Mater.* **9**(2) (1975) 157.
7. S. G. LEKHNITSKII, "Anisotropic Plates," Gordon And Breach Science Publishers, 1968.
8. B. N. NGUYEN, *J.Comp. Mater.* **31** (1997) 1672.
9. R. J. NUISMER and J. M. WHITNEY, *Am. Soc. For Testing Mat.* (1975) 117.
10. I. SHAHID, F. K. CHANG and L. B. ILCEWICZ, *I.C.C.M. 9*, **5** (1993) 97.
11. I. SHAHID, F. K. CHANG and L. B. ILCEWICZ, *I.C.C.M. 9*, **V** (1993) 105.
12. J. M. WHITNEY and R. J. NUISMER, *J. Comp. Mat.* **8**, (1974) 253.

Received 15 October 2004
and accepted 02 August 2005